AGU PUBLICATIONS

Geophysical Research Letters

RESEARCH LETTER

10.1002/2015GL064150

Special Section:
Effects of the Comet C/2013 A1 (Siding Spring) meteor shower in 2014 on Mars atmosphere and ionosphere: Observations from MAVEN, Mars Express, and Mars Reconnaissance Orbiter

Effects of the passage of Comet C/2013 A1 (Siding Spring) observed by the Shallow Radar (SHARAD) on Mars Reconnaissance Orbiter

Marco Restano[1], Jeffrey J. Plaut[2], Bruce A. Campbell[3], Yonggyu Gim[2], Daniel Nunes[2], Fabrizio Bernardini[1], Anthony Egan[4], Roberto Seu[1], and Roger J. Phillips[5]

[1]Dipartimento DIET, Università di Roma "La Sapienza", Rome, Italy, [2]Jet Propulsion Laboratory, California Institute of Technology, Pasadena, California, USA, [3]Smithsonian Institution, Washington, District of Columbia, USA, [4]Space Operations Department, Southwest Research Institute, Boulder, Colorado, USA, [5]Planetary Science Directorate, Southwest Research Institute, Boulder, Colorado, USA

Key Points:
- The interaction of the Comet Siding Spring's materials with Mars' ionosphere
- Ions generated from the interaction created a temporary anomalous ionized layer

Supporting Information:
- Texts S1–S3, Figures S1–S5, and Table S1

Correspondence to:
M. Restano,
marco.res@inwind.it

Citation:
Restano, M., J. J. Plaut, B. A. Campbell, Y. Gim, D. Nunes, F. Bernardini, A. Egan, R. Seu, and R. J. Phillips (2015), Effects of the passage of Comet C/2013 A1 (Siding Spring) observed by the Shallow Radar (SHARAD) on Mars Reconnaissance Orbiter, *Geophys. Res. Lett.*, *42*, 4663–4669, doi:10.1002/2015GL064150.

Received 7 APR 2015
Accepted 16 APR 2015

Abstract The close passage of Comet C/2013 A1 (Siding Spring) to Mars provided a unique opportunity to observe the interaction of cometary materials with the Martian ionosphere and atmosphere using the sounding radar SHARAD (SHAllow RADar) aboard Mars Reconnaissance Orbiter. In two nightside observations, acquired in the 10 h following the closest approach, the SHARAD data reveal a significant increase of the total electron content (TEC). The observed TEC values are typical for daylight hours just after dawn or before sunset but are unprecedented this deep into the night. Results support two predictions indicating that cometary pickup O^+ ions, or ions generated from the ablation of cometary dust, are responsible for the creation of an additional ion layer.

1. Introduction

The Oort-cloud Comet Siding Spring C/2013 A1 (CSS) was discovered on 3 January 2013 at Siding Spring Observatory and made its close encounter with Mars on 19 October 2014. The closest approach distance was around 139,500 km, less than a third of the Earth-Moon distance. Images taken by the High Resolution Imaging Science Experiment camera on NASA's Mars Reconnaissance Orbiter showed that the comet's nucleus was between 400 and 700 m in diameter. Regarded as icy small solar system bodies, comets heat up and outgas when passing close to the Sun. The volatile materials within the comet sublimate and stream out of the nucleus, carrying dust away. The cometary coma, composed of dust and gas, was expected to impinge upon the upper atmosphere of Mars for about 1 h [*Yelle et al.*, 2014; *Tricarico et al.*, 2014; *Kelley et al.*, 2014], providing a unique opportunity to infer the physical consequences of the passage of a planet through a cometary coma. Preliminary investigations predicted considerable variations in the atmospheric constituents [*Yelle et al.*, 2014] and the temporary formation of a new ion layer [*Gronoff et al.*, 2014; *Withers*, 2014]. According to *Gronoff et al.* [2014], the cometary pickup O^+ ion precipitation was expected to be a significant nightside ionization source, originating from photo-dissociated H_2O molecules from the comet. The ablation of interplanetary dust in a planetary upper atmosphere introduces metal species into the atmosphere [*Withers*, 2014; *Grebowsky et al.*, 2002]. *Withers* [2014] provided a relationship between properties of the dust population of the cometary coma and density of metal species in the atmosphere and ionosphere of Mars. The study focused on Mg, as it is abundant, readily ionized, and otherwise absent from the Martian upper atmosphere [*Pesnell and Grebowsky*, 2000]. Dust particles will ablate entering the atmosphere at orbital speeds. The Mg^+ ion is generated from impact ionization. *Withers* [2014] neglected ions produced from Mg atoms by photoionization or charge exchange and assumed the impact ionization to be the dominant ionization source for high-speed meteors like Comet Siding Spring. *Withers* [2014] predicted a subsequent increase of the density of metal ions of more than an order of magnitude. Such an event should lead to a drastic change in the structure of the lower ionosphere, and the Mg^+ lifetime was predicted to be hours to days. The comet activity, modeled as a flux of mass and energy, and the solar activity at the time of the encounter were indicated as key factors in all these predictions [*Yelle et al.*, 2014; *Gronoff et al.*, 2014; *Withers*, 2014]. Among the instruments operating in Mars orbit, the Shallow Radar (SHARAD) and the Mars Advanced Radar for Subsurface and Ionospheric Sounding (MARSIS) provide information regarding the Martian ionosphere. Instruments on board the Mars

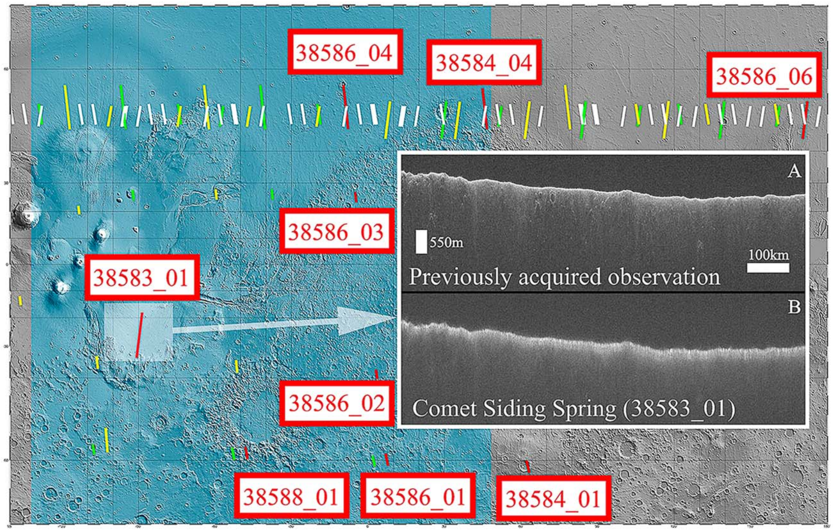

Figure 1. Map showing the planned observations for latitudes between 70°N and 70°S. The red color shows observations acquired in the first 12 h after the closest approach time; the green color shows those acquired from 12 to 0 h before the closest approach time; and the yellow color shows those acquired from 12 to 24 h after the closest approach time. Other observations are reported in white. The red-colored observations are identified with both the orbit (3858X) and the observation number (_0X). The region in blue represents the area predicted to be most influenced by the cometary material [*Tricarico et al*. 2014]. The white square encloses the nighttime observation 38583_01 acquired on Solis Planum roughly 2.5 h after the comet's passage. The influence of the comet is clearly visible in (b) the second radargram, which appears blurry because of the increase of the TEC when compared to (a) a nighttime observation acquired 1 year previously unaffected by ionospheric distortion. (*Map credit*: Mars Orbiter Laser Altimeter Science Team.)

Atmosphere and Volatile Evolution (MAVEN) spacecraft return information on the pickup ion densities and speeds, atmospheric neutrals and ions, and UV emission profiles. This paper focuses on SHARAD observations during Comet Siding Spring's passage.

2. The Shallow Radar

The Shallow Radar (SHARAD) is a subsurface sounding radar [*Croci et al*., 2011; *Seu et al*., 2007] provided by the Italian Space Agency for the NASA Mars Reconnaissance Orbiter mission. Principal objectives include the detection of liquid and solid water below the surface and the mapping of subsurface geologic structures. The spacecraft's orbit is nearly circular with an altitude between 255 km and 320 km. Thirteen orbits per day are performed. SHARAD operates in the high frequency band between 15 and 25 MHz, with a 10 MHz bandwidth that yields a free-space range resolution of 15 m. For each measurement, SHARAD transmits a short (85 μs) pulse within which the frequency sweeps from 15 MHz to 25 MHz. The pulse repetition interval is 1428 μs. Typical observations last from 60 s up to about 700 s. For a typical onboard pulse presumming of 4, ~10,000 to ~122,000 individual echoes are obtained. The transmitted radio wave leads to a significant penetration depth in low-conductivity materials such as dry soil and ice due to its long wavelength (15 m). After the initial encounter with the surface, the transmitted energy is partially reflected back to the receiver and partially transmitted into the subsurface. The largest reflection typically occurs at the Martian surface [*Seu et al*., 2004], while other interfaces, such as layered ice deposits in the subsurface, produce smaller reflections related to contrasts in the electrical properties, as well as attenuation of the signal (path loss). SHARAD data [*Seu et al*., 2004] reveal subsurface structures with a great amount of detail when radio wave propagation is facilitated by the medium (e.g., low dielectric and magnetic losses). The along-track resolution after on-ground synthetic aperture radar (SAR) processing ranges from 300 m to 1000 m. Images showing the surface and subsurface profiles along the orbit track are known as radargrams (Figure 1a).

The ionosphere [*Safaeinili et al*., 2003] induces attenuation and distortion in the propagating signals due to its complex refractive index. The attenuation is due to the electron collisions with the neutrals and ions, and the signal distortion is due to the frequency dependence of the refractive index. The plasma frequency is related to the electron density $N_e(z)$ (m^{-3}) by $f_p(z) = 8.98\sqrt{N_e(z)}$, whereas the complex refractive index is equal to $\eta^2 = 1 - \frac{f_p^2(z)}{f^2 - jfv}$, where v is the collision frequency and z is the height. The induced distortion causes an overall delay and a frequency-dependent phase dispersion given by $\Delta\varphi(f) = -\frac{4\pi f}{c_0}\int_{z_0}^{z_1}\mathrm{real}(\eta - 1)\,dz$, where f is the signal frequency and z_0 and z_1 are the lower and upper limits of the ionosphere where the signal propagates. The dispersion leads to a blurred radar image (Figure 1b).

The magnitude of dispersion depends on the ionized particle density, mostly electrons, integrated over the propagation path. The density is related to the total electron content $\mathrm{TEC} = \int N_e(z)dz$. The TEC is a basic characterization of the ionosphere, giving the total number of electrons in a 1 m square column between the spacecraft and the surface of Mars. The TEC can be estimated by applying frequency- and TEC-dependent correction factors during ground data processing. When properly corrected [*Campbell et al.*, 2014; *Safaeinili et al.*, 2007], the radargram is sharply focused at the expected time delay. Attenuation of the signal due to the ionosphere increases as the frequency decreases, but SHARAD operates well above the plasma frequency and total attenuation is relatively low. SHARAD is not capable of revealing the height of ion layers as the transmitted frequencies are significantly higher than the plasma frequency, which typically varies from 800 kHz (deep night) to around 2.8 MHz (noon). MARSIS, whose range of frequencies is between 0.1 MHz and 5.5 MHz, can provide this information as its signal is reflected when the electron plasma frequency is equal to the transmitted frequency [*Picardi et al.*, 2004].

3. The Planning of the Observations

In our investigation, the SHARAD was not used for sounding the subsurface, but instead, it focused on the search, using the dispersion and delay of the surface radar echo, for anomalies in the TEC due to interactions between the cometary materials and the Martian atmosphere. Because the nominal ionosphere electron density is primarily dependent upon solar irradiation, described in terms of solar zenith angle (SZA), a crucial point of the analysis was the planning of observations at desirable SZAs while also considering that other instruments on board the orbiter were involved in the study of the comet's passage. The first step was to consider the area most influenced by the cometary debris. This region was identified by *Tricarico et al.* [2014] and is reported in blue in Figure 1 along with a plot of the planned observations. Temporal variations of the ionospheric electron density due to the comet's passing were anticipated; *Yelle et al.* [2014] predicted that the variation of hydrogen in the atmosphere could persist for tens of hours; *Withers* [2014] predicted that enhanced metal ion densities could persist for hours to days; and *Gronoff et al.* [2014] indicated the temporary creation of an extra ionospheric layer at 110 km altitude. For this reason, we planned the observations over a time window starting 2 days before the closest approach (19 October 2014) and finishing 2 days after. This approach was taken both to follow the possible temporal variations of the ionospheric electron density and to create different groups of observations at a variety of SZA values, which facilitated subsequent comparisons between observations collected with and without the comet's presence. As long as the radar receives a surface echo with a sufficient signal-to-noise level, models can be used to compensate distortions and estimate ionospheric parameters. A set of 127 observations was planned and executed, avoiding regions of strong crustal magnetic fields or severe surface roughness that could hamper or bias the results. In particular, 13 observations were collected during four orbits in the 12 h following the closest approach which occurred on 19 October 2014 at 18:28 UTC. Observations collected at latitudes between 70°N and 70°S are shown in red in Figure 1. Additional observations were made in the polar regions. The first observation following closest approach, 38583_01, was acquired on 19 October 2014 at 21:05 UTC and had a duration of 300 s. The second orbit, 38584, started at 23:28 UTC and included four 60 s observations and one 180 s observation (38584_04). The third orbit, 38586, started on 20 October 2014 at 03:13 UTC and included four 60 s observations and two 180 s observations (38586_04 and _06). The fourth orbit, 38588, started at 07:00 UTC and included a single 60 s observation (38588_01). The majority of the observations belong to three groups having SZA around 80°, 93°, and 120°, respectively. The long time window combined with these groups of observations permits analysis of the temporal extent of cometary influence on the Martian atmosphere and ionosphere.

4. Results

Enhancements over the typical total electron content were found in two nighttime observations acquired in the 12 h following the comet's passage, during two different orbits. The closest approach point was reached by the comet on 19 October 2014 at 18:28 UTC. SHARAD began post-CSS observations around 1 h after the expected peak of cometary dust reaching Mars [*Tricarico et al.*, 2014]. The duration of the influence of cometary dust was predicted to be hours to days [*Withers*, 2014]. The first observation, 38583_01, was acquired at 21:05 UTC over the smooth volcanic plains of Solis Planum. The average SZA was 113°, deep into the night, and the location of the observation is near the center of the hemisphere of Mars predicted to receive maximum dust flux (shaded region in Figure 1). The resulting radargram, when processed with normal parameters for nightside observations (i.e., no correction of phase distortion), shows a smeared surface echo indicative of dispersion of the radar pulse by the ionosphere (Figure 1b). This is a highly unusual occurrence for nightside SHARAD passage. A nightside pass over the same track taken a year earlier with an average SZA of 140° shows no such dispersion (Figure 1a). Similarly, all the planned nightside passes (SZA~110°–120°) of the comet observation campaign that were acquired before the comet's passage have no such signature. In fact, such an effect has never been observed in hundreds of previous nightside SHARAD observations. A second nighttime observation, 38586_05, showing a similar feature, was collected on 20 October 2014 at 03:54 UTC near the North Pole. No other SHARAD CSS observations reveal unusual ionospheric behavior. TEC enhancements were found in two regions in the area indicated by *Tricarico et al.* [2014], suggesting that a persistent layer was present during the 10 h following the closest approach.

As the number of electrons per unit volume [*Kelly*, 2012] should be approximately equal to the number of positive ions of all types $N_e \cong \sum_{\text{ions}} N_i^+$, SHARAD measurements agree with predictions made by *Withers* [2014] and by *Gronoff et al.* [2014]. *Withers* [2014] related the ablation of cometary dust particles both to a temporary increase of the density of metal ions (Mg^+) and to a drastic change in the structure of the lower ionosphere. *Gronoff et al.* [2014] indicated the temporary creation of an extra ionospheric layer and suggested a close monitoring of the electron density at 110 km. According to *Gronoff et al.* [2014], the cometary pickup O^+ ion precipitation was expected to be a significant nightside ionization source, originating from photo-dissociated H_2O molecules from the comet. SHARAD is not capable of detecting either the height of the temporary ion layer or the ion species; however, MARSIS and instruments onboard MAVEN were able to provide additional information. MARSIS detected an enhanced region of ionization at the North Pole near 100 km altitude about 2.5 h before the SHARAD observation 38586_05 [*Gurnett et al.*, 2015]. Measurements made from ~10 h to 2.5 days after the passage of CSS by the Neutral Gas and Ion Mass Spectrometer onboard MAVEN revealed at least 12 species of positive metal ions [*Benna et al.*, 2015]. MAVEN's Imaging Ultraviolet Spectrograph observed ultraviolet emission from Mg^+ and Fe^+ ions in the Martian atmosphere for several hours after the closest approach [*Schneider et al.*, 2015].

Three independent approaches were used to calculate the TEC values from SHARAD observations affected by the comet. The approach adopted by the Italian team of the Dipartimento di Ingegneria dell'Informazione, Elettronica e Telecomunicazioni (DIET) of Sapienza University of Rome corrected the ionosphere distortion on individual echoes without applying SAR processing (see Text S1 in the supporting information). This correction scheme is described in *Restano et al.* [2014] and supposes an ionosphere layer having a constant plasma frequency value that is estimated, along with the additional time delay, by maximizing the amplitude of the range-compressed SHARAD surface echo. The TEC value is calculated from the ionospheric time delay as indicated in *Garner et al.* [2008].

Similarly, the TEC is routinely estimated as part of the processing of U.S. SHARAD team products delivered to the Planetary Data System. This processing (see Text S2 in the supporting information) uses an autofocusing approach to maximize the sharpness of surface echoes in data blocks that are typically 10–20 s long (35 to 70 km along track). The phase distortion parameter in this model, initially derived from empirical analyses [*Campbell et al.*, 2011], has been found to correlate well with the ionosphere-induced round-trip time delay of the radar echoes [*Campbell et al.*, 2014] and thus with the TEC. Comparison of the surface location at cross-over points from hundreds of focused radargrams, collected under different ionospheric conditions, shows that these TEC estimates are very robust.

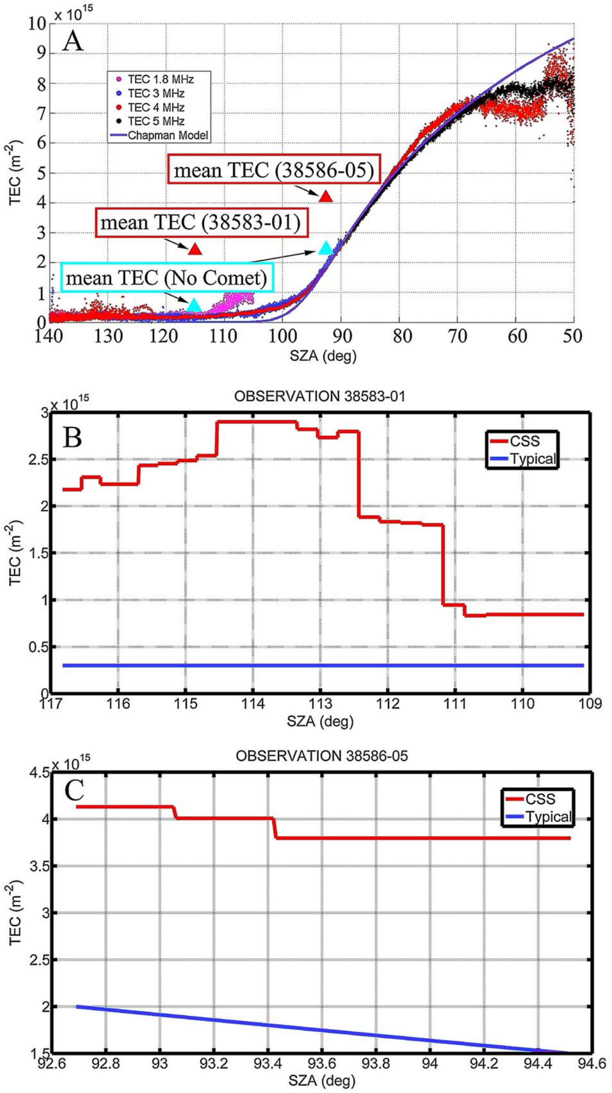

Figure 2. (a) Total electron content (TEC) as a function of SZA derived from thousands of observations by MARSIS [*Cartacci et al.*, 2013]. Nightside is SZA > 90; dayside is SZA < 90. The red triangles show SHARAD values from observations affected by Comet Siding Spring. The mean value of the TEC estimates produced by the three approaches is shown (see Texts S1–S3 in the supporting information) and is plotted at the mean SZA value of each observation. The cyan triangles show SHARAD values from observations not affected by Comet Siding Spring (see Text S1 in the supporting information). Such values are in good agreement with MARSIS TEC estimates over the 2006–2010 period [*Cartacci et al.*, 2013]. (b) TEC enhancement for the first observation of interest (38583_01), showing significant spatial variation. (c) TEC enhancement for the second observation of interest (38586_05).

In the approach adopted by the Jet Propulsion Laboratory to estimate the TEC (see Text S3 in the supporting information), the total electron density was scanned and the strength of surface returns monitored. The maximum surface return is expected when a correct electron density is used. Pulse-by-pulse optimization shows the statistical variation of the total electron density. Moreover, radargrams were also generated and compared using different electron density parameters. Unlike the pulse-by-pulse comparison, a constant total electron density for all the pulses for each radargram has been applied. Both methods are in good agreement.

Results obtained by the three approaches are consistent (see Texts S1–S3 in the supporting information). The mean value of the TEC estimates produced by the three approaches is shown for each observation in Figure 2 along with typical TEC values estimated by MARSIS for different SZA values [*Cartacci et al.*, 2013]. For a single observation, the mean TEC value is determined by averaging the TEC values retrieved either from each individual echo composing the observation (see Text S1 in the supporting information) or from a block of echoes (see Texts S2 and S3 in the supporting information). The three approaches differ in the way they process the individual echoes. The mean values shown in Figure 2 can be compared to typical TEC values, as the TEC values are typically constant both for SZA >110° (nighttime) and for observations of short duration. To illustrate the spatial variation during single observations, the TEC enhancement along the two observations of interest is shown in Figures 2b and 2c. No significant variation in the SHARAD signal attenuation has been revealed, although such changes are relatively modest in any case [*Campbell et al.*, 2014]. The first observation of interest, 38583_01, lasted 300 s and consisted of 52173 individual echoes. The measured ionosphere in terms of total electron content is 5 to 10 times, which is measured at these times of night during previous SHARAD observations (see Texts S1–S3 in the supporting information). The estimated TEC (Figure 2b) increases to a maximum TEC of ~3e15 m^{-2} as the SZA decreases from 117° to 114°, then is observed to decline abruptly as the track ends its coverage near a SZA of about 109° (see Text S2 in the supporting information).

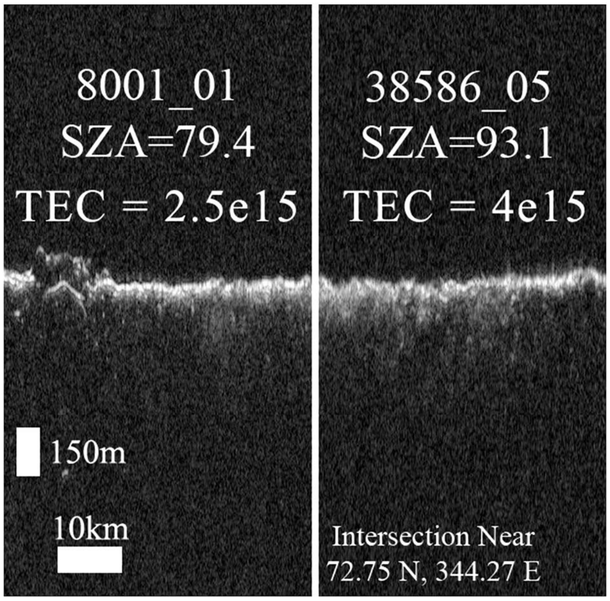

Figure 3. Close correspondence of the surface delay position between observation 38586_05 and observation 8001_01. This comparison validates the estimate of the TEC during the comet's close approach to Mars.

This excursion in TEC occurred over a lateral distance of about 600 km. The pulse-by-pulse optimization approach adopted by the Jet Propulsion Laboratory indicate a possible maximum TEC of ~4e15 m^{-2} (see Text S3 in the supporting information).

For the comet observation during SHARAD track 38586_05, it is possible to compare the calculated TEC and associated delay correction with those applied to a previous dayside track 8001_01 near their cross-over point at 72.75°N, 344.27°E (Figure 3). The close correspondence of the surface delay position at the intersection of these radargrams validates our estimate of the TEC during the comet's close approach to Mars. This observation shows a 1.6 to 2 times TEC enhancement with respect to typical SHARAD observations having a similar SZA (see Texts S1–S3 in the supporting information). The estimated TEC is quite stable along the observation (Figure 2c), which is composed of 10,070 individual echoes and lasts only 60 s. The observed TEC values are typical for daylight hours just after dawn or before sunset but are unprecedented for the nightside SZAs of these post-CSS observations (Figure 2a).

5. Conclusions

The SHARAD was successfully operated during the passage of Comet C/2013 A1 (Siding Spring) at Mars. The use of SHARAD was motivated by studies indicating the possible production of a temporary ion layer created by the interaction between cometary materials and the upper atmosphere of Mars. An extensive set of observations was planned and executed to detect possible temporal variations of the ionospheric electron density. Results indicate that the nightside developed a highly anomalous ionized layer that was observed twice in the 10 h following the comet's closest approach. The two observations of interest belong to different orbits separated by a time span of 7 h and were collected south of the equator and near the north pole, respectively. The TEC enhancement is time varying in the first observation of interest where significant variability in the TEC was observed over a short distance and small interval of SZA. In the second observation of interest, much shorter in duration, the TEC enhancement is relatively stable. The nightside TEC enhancements have never been observed in hundreds of previous radar observations. The obtained results support both predictions and investigations performed by MARSIS, NGIMS and IUVS during Comet Siding Spring's passage.

Acknowledgments
The Shallow Subsurface Radar (SHARAD) was provided by the Italian Space Agency (ASI), and its operations are led by the DIET Department, University of Rome "La Sapienza" under an ASI science contract. The Mars Reconnaissance Orbiter mission is managed by the Jet Propulsion Laboratory, California Institute of Technology, for the NASA Science Mission Directorate, Washington, DC. SHARAD data become available on the Geosciences Node of NASA's Planetary Data System (http://pds-geosciences.wustl.edu/) 6 months after the collection of the observations.

The Editor thanks Joseph Grebowsky and an anonymous reviewer for their assistance in evaluating the paper.

References

Benna, M., P. Mahaffy, J. Grebowsky, J. Plane, R. Yelle, and B. Jakosky (2015), Metallic ions in the upper atmosphere of Mars from the passage of comet Siding Spring, *Geophys. Res. Lett.*, doi:10.1002/2015GL064159.

Campbell, B. A., N. E. Putzig, L. M. Carter, and R. J. Phillips (2011), Autofocus correction of phase distortion effects on SHARAD echoes, *IEEE Geosci. Remote Sens. Lett.*, doi:10.1109/LGRS/2011.2143692.

Campbell, B. A., N. Putzig, F. J. Foss, and R. J. Phillips (2014), SHARAD signal attenuation and delay offsets due to the Martian ionosphere, *IEEE Geosci. Remote Sens. Lett.*, *11*, doi:10.1109/LGRS.2013.2273396.

Cartacci, M., et al. (2013), Mars ionosphere total electron content analysis from MARSIS subsurface data, *Icarus*, *223*, doi:10.1016/j.icarus.2012.12.011.

Croci, R., R. Seu, E. Flamini, and E. Russo (2011), The Shallow Radar (SHARAD) on board the NASA MRO mission, *Proc. IEEE*, *99*, doi:10.1109/JPROC.2010.2104130.

Garner, T. W., T. L. Gaussiran, B. W. Tolman, R. B. Harris, R. S. Calfas, and H. Gallagher (2008), Total electron content measurements in ionospheric physics, *Adv. Space Res.*, *42*, doi:10.1016/j.asr.2008.02.025.

Grebowsky, J. M., J. I. Moses, and W. D. Pesnell (2002), Meteoric material—An important component of planetary atmospheres, in *Atmospheres in the Solar System: Comparative Aeronomy*, *Geophys. Monogr. Ser.*, vol. 130, edited by M. Mendillo, A. F. Nagy, and J. H. Waite, pp. 235–244, AGU, Washington, D. C.

Gronoff, G., A. Rahmati, C. S. Wedlund, C. J. Mertens, T. E. Cravens, and E. Kallio (2014), The precipitation of keV energetic oxygen ions at Mars and their effects during the comet Siding Spring approach, *Geophys. Res. Lett.*, *41*, 4844–4850, doi:10.1002/2014GL060902.

Gurnett, D. A., D. D. Morgan, A. M. Persoon, L. J. Granroth, A. J. Kopf, J. J. Plaut, and J. L. Green (2015), An ionized layer in the upper atmosphere of Mars caused by dust impacts from comet Siding Spring, *Geophys. Res. Lett.*, doi:10.1002/2015GL063726.

Kelley, M. S. P., T. L. Farnham, D. Bodewits, P. Tricarico, and D. Farnocchia (2014), A study of dust and gas at Mars from Comet C/2013 A1 (SIDING SPRING)", *Astrophys. J. Lett.*, *792*, doi:10.1088/2041-8205/792/1/L16.

Kelly, M. C. (2012), *The Earth's Ionosphere: Plasma Physics and Electrodynamics*, Academic Press, Elsevier, London.

Pesnell, W. D., and J. Grebowsky (2000), Meteoric magnesium ions in the Martian atmosphere, *J. Geophys. Res.*, *105*, 1695–1707, doi:10.1029/1999JE001115.

Picardi, G., et al. (2004), MARSIS: Mars Advanced Radar for Subsurface and Ionosphere Sounding, Mars Express: The scientific payload, ESA Report SP-1240, European Space Agency Publication Division, Noordwijk, Netherlands.

Restano, M., G. Picardi, and R. Seu (2014), 1D-FDTD characterization of ionosphere influence on ground penetrating radar data inversion, *IEEE Trans. Antennas Propag.*, *62*, doi:10.1109/TAP.2014.2299825.

Safaeinili, A., W. Kofman, J. F. Nouvel, A. Herique, and R. L. Jordan (2003), Impact of Mars ionosphere on orbital radar sounder operation and data processing, *Planet. Space Sci.*, *51*, doi:10.1016/S0032-0633(03)00048-5.

Safaeinili, A., et al. (2007), Estimation of the total electron content of the Martian ionosphere using radar sounder surface echoes, *Geophys. Res. Lett.*, *34*, L23204, doi:10.1029/2007GL032154.

Schneider, N. M., et al. (2015), MAVEN IUVS observations of the aftermath of the comet Siding Spring meteor shower on Mars, *Geophys. Res. Lett.*, doi:10.1002/2015GL063863.

Seu, R., et al. (2004), SHARAD: The MRO 2005 shallow radar, *Planet. Space Sci.*, *52*, doi:10.1016/j.pss.2003.08.024.

Seu, R., et al. (2007), SHARAD sounding radar on the Mars Reconnaissance Orbiter, *J. Geophys. Res.*, *112*, E05S05, doi:10.1029/2006JE002745.

Tricarico, P., et al. (2014), Delivery of dust grains from comet C/2013 A1 (Siding Spring) to Mars, *Astrophys. J. Lett.*, *787*, doi:10.1088/2041-8205/787/2/L35.

Withers, P. (2014), Predictions of the effects of Mars's encounter with comet C/2013 A1 (Siding Spring) upon metal species in its ionosphere, *Geophys. Res. Lett.*, *41*, 6635–6643, doi:10.1002/2014GL061481.

Yelle, R. V., A. Mahieux, S. Morrison, V. Vuitton, and S. M. Hörst (2014), Perturbation of the Mars atmosphere by the near-collision with Comet C/2013 A1 (Siding Spring), *Icarus*, *237*, doi:10.1016/j.icarus.2014.03.030.